Pc5 wave power in the quiet-time plasmasphere and trough: CRRES observations

Michael Hartinger,[1] Mark B. Moldwin,[1,2] Vassilis Angelopoulos,[1] Kazue Takahashi,[3] Howard J. Singer,[4] Roger R. Anderson,[5] Yukitoshi Nishimura,[6,7] and John R. Wygant[8]

[1]   The Combined Release and Radiation Effects Satellite (CRRES) mission provides an opportunity to study the distribution of MHD wave power in the inner magnetosphere both inside the high-density plasmasphere and in the low-density trough. We present a statistical survey of Pc5 power using CRRES magnetic field, electric field, and plasma wave data separated into plasmasphere and trough intervals. Using a database of plasmapause crossings, we examined differences in power spectral density between the plasmasphere and trough regions. These differences were typically a factor of 3 or 4 but could be as much as an order of magnitude and could be seen in both electric and magnetic field data. Our study shows that determining the plasmapause location is important for understanding and modeling the MHD wave environment in the Pc5 frequency band. **Citation:** Hartinger, M., M. B. Moldwin, V. Angelopoulos, K. Takahashi, H. J. Singer, R. R. Anderson, Y. Nishimura, and J. R. Wygant (2010), Pc5 wave power in the quiet-time plasmasphere and trough: CRRES observations, *Geophys. Res. Lett.*, *37*, L07107, doi:10.1029/2010GL042475.

1.   Introduction

[2]   The Earth's magnetosphere supports standing magnetohydrodynamic (MHD) waves, which include field line resonances (FLR) and cavity resonances [*Kivelson and Southwood*, 1985]. The magnetosphere can also be a waveguide for MHD waves [*Samson et al.*, 1992]. The structure and location of the plasma density gradient of the outer boundary of the plasmasphere, or plasmapause, as well as the distribution of plasma density within the plasmasphere, affect the transmission of wave energy into the plasma-

sphere and determine the properties of standing waves [*Lee and Takahashi*, 2006].

[3]   Pc5 waves have frequencies from approximately 2 to 7 mHz and are strongly controlled by variations in the solar wind [*Takahashi and Ukhorskiy*, 2007]. These waves are also generated through processes internal to the Earth's magnetosphere [*Chen and Hasegawa*, 1991]. The Pc5 frequency band is important because MHD waves near these frequencies may accelerate energetic electrons in the outer radiation belts through drift resonance [*Elkington et al.*, 2003].

[4]   Previous statistical studies have typically not differentiated between the high-density plasmasphere and low-density trough region. For example, *Hudson et al.* [2004] found occurrence rates of Pc5 FLRs using CRRES magnetometer data, but they did not specify whether the observed FLRs occurred in the plasmasphere or trough region. *Brautigam et al.* [2005] obtained radial profiles of electric field power spectral densities (PSDs) using CRRES, but they did not make comparisons between the plasmasphere and trough. We present a statistical comparison of Pc5 wave power between the trough and plasmasphere using fluxgate magnetometer, electric field instrument, and sweep frequency receiver data from CRRES. We compare power in both regions to examine the plasmasphere's role in modulating Pc5 wave activity.

2.   Instrumentation

[5]   CRRES operated from 25 July 1990 to 12 October 1991 in a geosynchronous transfer orbit. The orbit was designed so the local time at apogee changed by 2.5 minutes per day for complete local time coverage over 19 months. Since the mission ended in less than 15 months, there is a gap in coverage at higher L on the dayside. CRRES had a spin period of about 30 seconds [*Johnson and Kierein*, 1992].

[6]   The CRRES plasma wave experiment included an electric dipole antenna and sweep frequency receiver. The upper hybrid resonance frequency and electron plasma frequency are obtained from plasma wave spectra. These frequencies can then be used to calculate electron density [*Anderson et al.*, 1992].

[7]   The CRRES triaxial fluxgate magnetometer was sensitive to magnetic field variations greater than 0.43 nT in high-gain mode and 22 nT in low-gain mode. For the present MHD wave study, only the high-gain data are useful. The gain mode switched when the magnetic field strength exceeded 850 nT, which occurs near 3.5 Re [*Singer et al.*, 1992]. The CRRES magnetometer data used in this

[1]Earth and Space Sciences Department, University of California, Los Angeles, California, USA.
[2]Atmospheric, Oceanic and Space Sciences Department, University of Michigan, Ann Arbor, Michigan, USA.
[3]Johns Hopkins University Applied Physics Laboratory, Laurel, Maryland, USA.
[4]NOAA Space Weather Prediction Center, Boulder, Colorado, USA.
[5]Physics and Astronomy Department, University of Iowa, Iowa City, Iowa, USA.
[6]Atmospheric and Oceanic Sciences Department, University of California, Los Angeles, California, USA.
[7]Solar Terrestrial Environment Laboratory, Nagoya University, Nagoya, Japan.
[8]School of Physics and Astronomy, University of Minnesota, Minneapolis, Minnesota, USA.

study were transformed from spacecraft coordinates into spin resolution data in a modified GSE coordinate system (MGSE), where x points along the CRRES spin axis, which is approximately parallel to the x-axis in GSE, y intersects the ecliptic and spin planes and points towards dusk, and z completes the set [*Brautigam et al.*, 2005]. These coordinates are similar to GSE because the CRRES spin axis points approximately nine degrees from the Earth-Sun line.

[8] The CRRES electric field instrument (EFI) measured the electric potential differences between two spherical probes and two cylindrical probes [*Wygant et al.*, 1992]. Both measurements were made in the spin plane of CRRES and yielded electric field measurements with a sensitivity of 0.1 mV/m. The third component along the spin axis was obtained by assuming E · B = 0. The spin-fit electric field data, like the magnetic field data, were transformed into MGSE. CRRES EFI data were previously used for statistical studies of electric field PSD in the Pc5 frequency band [*Brautigam et al.*, 2005]. We follow the same procedure as *Brautigam et al.* [2005] in selecting electric field data that can be used in the present study. Because of several restrictions on the CRRES EFI data, coverage is very limited [*Brautigam et al.*, 2005].

3. Data Processing

[9] Small gaps in the magnetometer and electric field data were filled through interpolation. A digital filter designed to pass frequencies below 2 mHz was applied. The low-pass filtered data were subtracted from the original data to remove the background field. The unprocessed and detrended data were both visually inspected for large spikes and unphysical wave activity, which were flagged. Step changes in any component, possibly due to current sheet crossings, were also flagged because they could be mistaken for Pc5 wave power in the statistical study.

[10] A running 32 point (16 minute) Fast Fourier Transform (FFT) with a half window overlap was applied to compute PSD. The *Tsyganenko*, 1989 model was used to compute the McIlwain L parameter for the time at the center of each FFT window [*McIlwain*, 1961; *Tsyganenko*, 1989].

[11] *Moldwin et al.* [2002] used electron density inferred from the CRRES sweep frequency receiver and the following criteria to identify the plasmapause boundary: the plasmapause occurs at the innermost location where there is at least a factor of five change in electron density within 0.5 L [*Moldwin et al.*, 2002]. Using these criteria, two plasmapause boundaries could be identified for each CRRES orbit. We compared the database of crossing times with the times at the center of each FFT window. If an FFT window occurred within 8.5 minutes of a crossing, it was identified as being at the plasmapause. If CRRES was outbound and an FFT window occurred 8.5 minutes or more before a crossing, it was flagged as the plasmasphere; if it was outbound and an FFT window occurred 8.5 minutes or more after a crossing, it was flagged as the trough. Similar criteria were used when CRRES was inbound. If there was no crossing identified on the inbound or outbound part of CRRES's orbit, the data were excluded. Only data flagged as plasmasphere or trough were used in the study.

[12] Data coverage is limited in certain regions in this study (see auxiliary material for Figure S1) for several reasons: there are large data gaps on the dayside because of

the early termination of the CRRES mission, CRRES spends more time at higher L values because of its lower radial velocity near the apogee, and CRRES preferentially samples high magnetic latitudes at high L.[1] Since some standing waves may have nodes in either the electric or magnetic field at certain latitudes, we use both electric and magnetic field data in the present study. However, the fluxgate magnetometer and EFI have unique limitations in data coverage. The magnetic field is poorly sampled for L less than 3.5 because only high-gain magnetometer data can be used. EFI also has many data coverage limitations [*Brautigam et al.*, 2005].

[13] Figure 1 is an example interval from an orbit used in this study. In the top panel, regions flagged as trough and plasmasphere are indicated. Electron density was used as a proxy for the plasma mass density when identifying the plasmapause. However, it is worth noting that trends in the electron density will not always track the plasma mass density, because the relative concentration of heavy ions may change in different regions [*Fraser et al.*, 2005].

[14] The second panel in Figure 1 shows the dawn-dusk component of the detrended electric field, and the third panel shows the dynamic power spectrum. The fourth and fifth panels are for the sunward component of the magnetic field. There is an enhancement in Pc5 activity visible in both the electric and magnetic field data beginning at 13:30 UT that appears to coincide with CRRES crossing the plasmapause and moving into the trough. In the present study, we used electric and magnetic field data from many such orbits to determine whether the plasmasphere plays a statistically significant role in modulating Pc5 wave activity.

4. Results

[15] The final data product used in this study is the total PSD, the sum of the PSD computed for all components in each FFT window, averaged over the 2 to 8 mHz frequency band. The data is binned by the *Tsyganenko*, 1989 L value. Some power data are below the noise threshold of the electric ($10^{-0.75}$ (mV/m)^2/Hz) and magnetic ($10^{0.52}$ nT^2/Hz) field instruments.

[16] We further bin the data by Kp and separate between quiet ($Kp \leq 3$) and active times ($Kp > 3$). Previous studies have shown that increased Kp is correlated with increased ULF wave power [*Takahashi and Anderson*, 1992]. Kp is also correlated with the most probable location of the plasmapause [*Moldwin et al.*, 2002]. There is a strong potential source of bias when measuring Pc5 wave power if we do not consider geomagnetic activity. For example, when Kp is low, the plasmapause is likely to be located at high L. Thus, CRRES is more likely to be inside the plasmasphere at high L for low Kp. Similarly, when Kp is high, the plasmapause is likely located at low L. Thus, CRRES is more likely to be in the trough at high L for high Kp. During strong geomagnetic storms, the inner magnetosphere can also become severely distorted, impacting field-line mapping and modulating field-line resonance frequencies, producing another source of bias related to Kp [*Berube et al.*, 2006]. Finally, there is a local time Kp bias on the spacecraft orbit due to the short duration of the CRRES mission. There was more

---

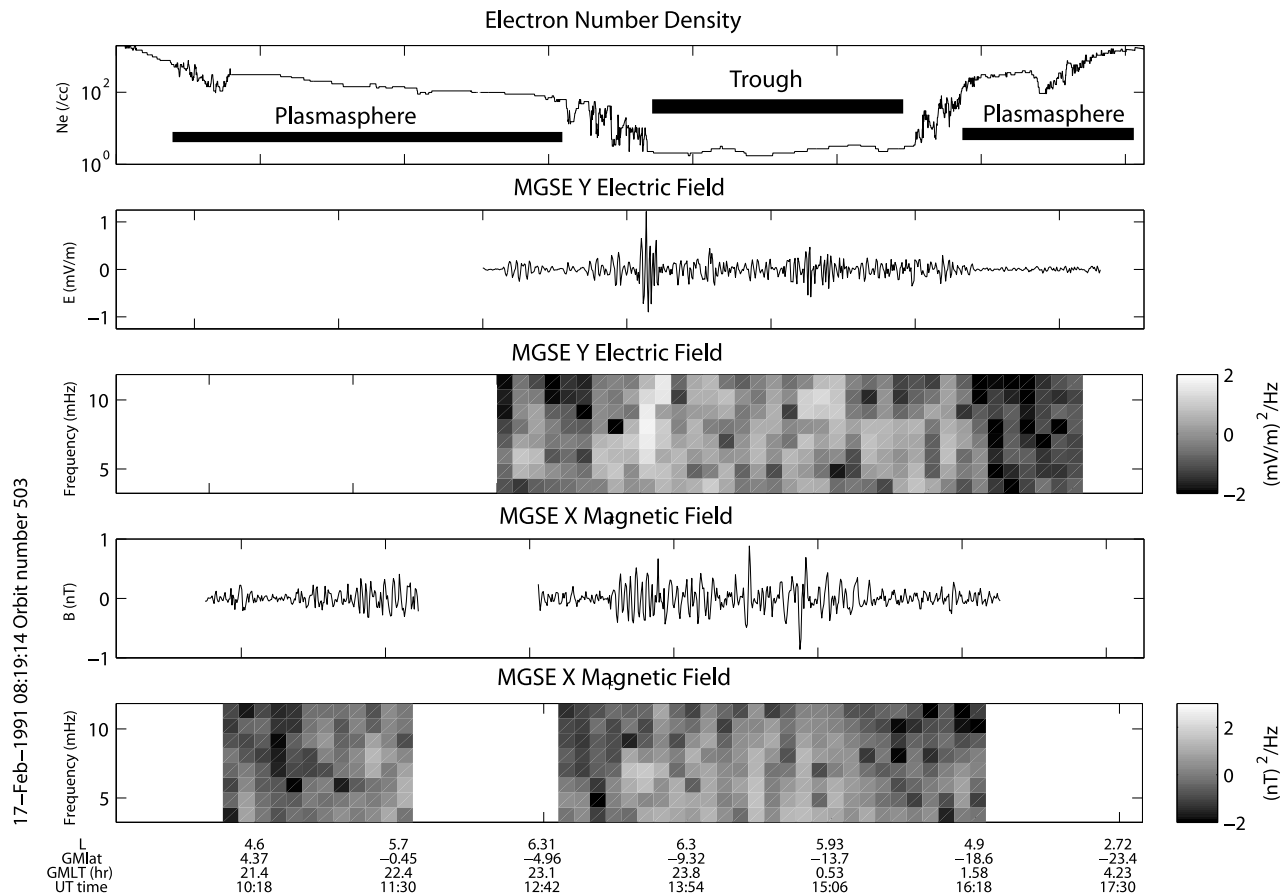[1]Auxiliary materials are available in the HTML. doi:10.1029/2010GL042475.

Figure 1. Orbit 503, 17 February 1991. An example of one orbit of CRRES data used in the statistical study. From top to bottom, electron density with plasmasphere and trough intervals indicated, MGSE y detrended electric field followed by corresponding dynamic power spectrum, MGSE x detrended magnetic field followed by corresponding dynamic power spectrum.

geomagnetic activity during the latter part of the CRRES mission, when the apogee was in the dusk and midnight sectors. Because these sources of bias were most evident for active times, we focus on results obtained for $Kp \leq 3$.

[17] Shown in Figure 2 are scatter plots of the logarithm of the Pc5 electric (left) and magnetic (right) field PSDs for all FFT windows in the midnight sector for quiet times. We plot the total power, or the sum of the power computed for
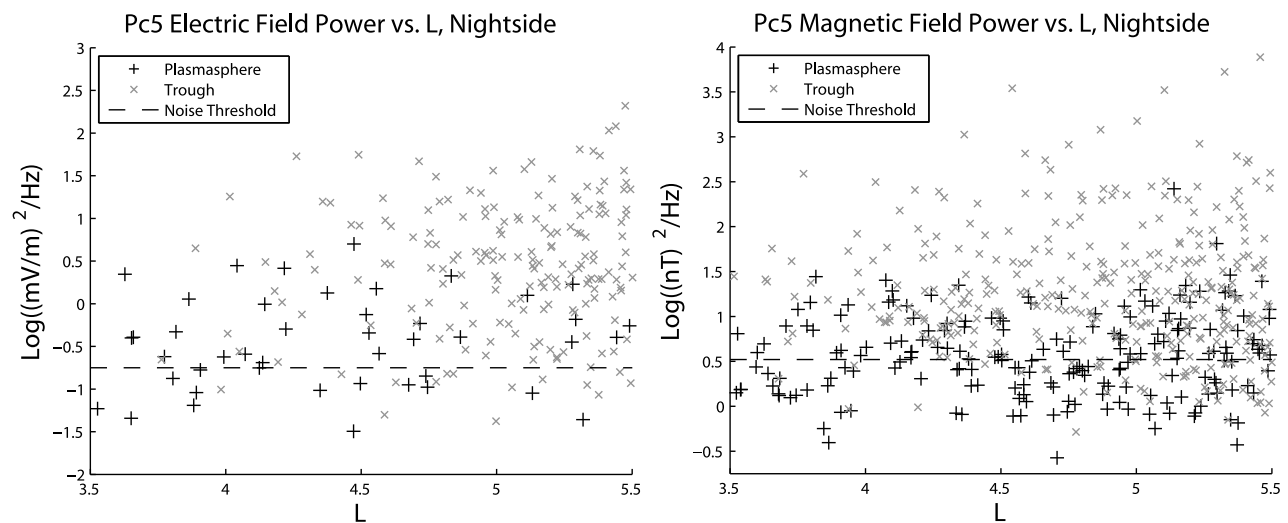

Figure 2. Scatter plots of total Pc5 power for each FFT window in the midnight sector (21 to 3 MLT) as a function of L. (left) Electric field data with the + symbol indicating plasmasphere data, the x symbol indicating trough data, and the dashed line indicating the noise threshold for the data. (right) The same symbols are used for magnetic field data.
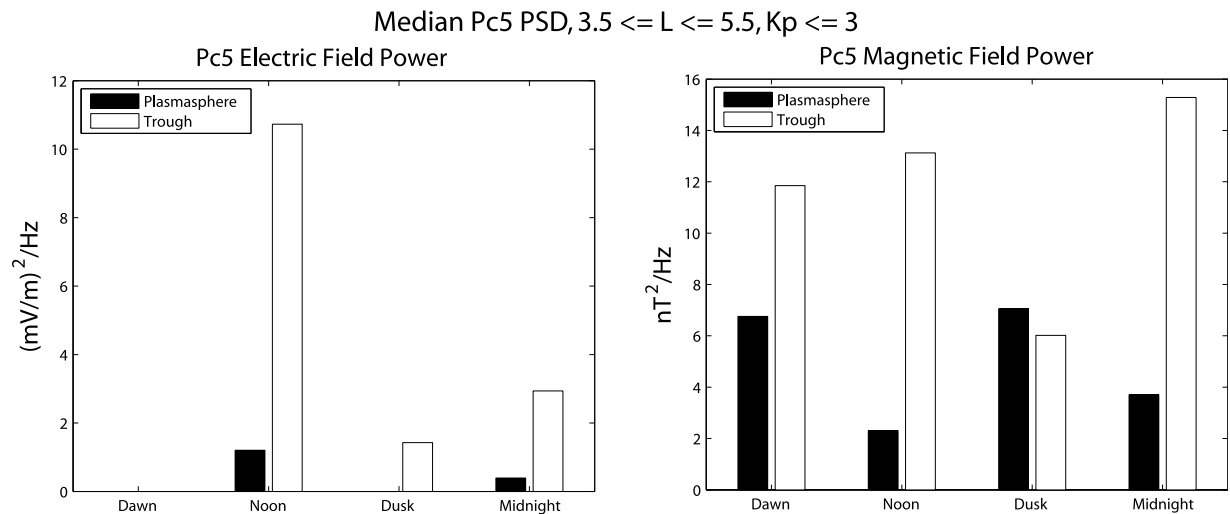
Median Pc5 PSD, 3.5 <= L <= 5.5, Kp <= 3

Figure 3. Median values of total electric and magnetic field power in the plasmasphere and trough in different MLT regions for intervals where Kp ≤ 3 and 3.5 ≤ L ≤ 5.5.

each component. We chose the midnight sector because of the good electric and magnetic field data coverage in both the plasmasphere and trough. The data are divided by region, with +'s representing plasmasphere data and x's representing trough data.

[18] A significant fraction of both the electric and magnetic field data recorded in the plasmasphere lie below the noise threshold of the instrument. The data also have a wide range, spanning more than three orders of magnitude for electric field data and four orders of magnitude for magnetic field data. In the present study, we will use median rather than mean values for comparisons, because the mean values can be strongly influenced by a few extreme events and a significant number of measurements below the noise threshold. The median electric field power value for all points in the plasmasphere is $10^{-0.41}$ $(mV/m)^2/Hz$ compared to $10^{0.47}$ $(mV/m)^2/Hz$ in the trough. The median magnetic field power value for all points in the plasmasphere is $10^{0.57}$ $(nT)^2/Hz$ compared to $10^{1.18}$ $(nT)^2/Hz$ in the trough. In both plots, the data in the plasmasphere are clustered at lower power values than the trough for all L.

[19] In Figure 3, we display the median power values for the electric (left) and magnetic (right) fields for different MLT sectors on a linear scale. Dawn is from 3 to 9 MLT, noon is from 9 to 15, dusk is from 15 to 21, and midnight is from 21 to 3. The data are further restricted to $Kp \leq 3$ and $3.5 \leq L \leq 5.5$, a particularly well sampled region for both electric and magnetic field data in the plasmasphere and trough.

[20] The only MLT sectors that allow comparisons between the plasmasphere and trough for both the electric and magnetic fields are noon and midnight. At midnight, the median power is roughly 8 times larger in the trough compared to the plasmasphere for the electric field and 4 times larger for the magnetic field. At noon, the median power is roughly 9 times larger in the trough compared to the plasmasphere for the electric field and 6 times larger for the magnetic field.

[21] In the dawn and dusk sectors, only magnetic field data is available for comparison. In the dawn sector, the total

magnetic field PSD is roughly twice as large in the trough compared to the plasmasphere. The dusk sector is the only local time sector where no significant difference in the magnetic field PSDs is observed between the plasmasphere and trough.

[22] We performed similar comparisons for L > 5.5 and $Kp > 3$ (see auxiliary material for Tables S1) and observed similar results. However, there was only adequate data for a comparison with both electric and magnetic field data in the midnight sector for L > 5.5. For both $Kp \leq 3$ and $Kp > 3$, we found that the trough had higher power than the plasmasphere by roughly an order of magnitude.

5. Discussion

[23] The most prominent feature in Figure 3 is the difference in the median PSDs between the trough and the plasmasphere. PSD may be lower in the plasmasphere because solar wind driven waves in the Pc5 band do not penetrate into the plasmasphere effectively. It is also possible that nominal conditions in the plasmasphere are not conducive to MHD resonance in the Pc5 band. If the fundamental FLR frequency and the fundamental cavity resonance frequency do not typically occur in the Pc5 band in the plasmasphere, one would expect a much lower average PSD.

[24] We find that the difference in PSDs between the plasmasphere and trough depends on local time sector. For example, we do not observe as significant a difference in the median magnetic field PSDs in the dusk sector compared to other sectors. There are a few possibilities for this local time dependence. It is possible that solar wind driven MHD waves in the Pc5 frequency band cannot penetrate into the plasmasphere effectively. Internally generated waves, however, may be more likely to occur inside the plasmasphere. This would explain the negligible difference in PSDs at dusk, as internally generated Pc5 waves are more likely to occur at dusk [*Hudson et al.*, 2004]. The distribution of the plasma mass density in the plasmasphere and the sharpness of the plasmapause density gradient also depend on local time and may play a role in determining the difference in

PSDs. For example, the dusk region is more structured due to the presence of plumes [*Moldwin et al.*, 2002].

6. Conclusions

[25] We have presented a statistical comparison of Pc5 wave power between the plasmasphere and trough regions and demonstrated that the plasmasphere plays a significant role in modulating Pc5 wave activity. For quiet times, the median total PSD in the electric and magnetic fields is higher in the trough compared to the plasmasphere. However, the difference in power depends on local time, with the largest differences of about an order of magnitude occurring at noon and midnight and almost no difference at dusk.

[26] Our observations and several previous observations and models have demonstrated the importance of constraining properties of the plasmasphere and plasmapause when studying MHD wave propagation and resonance in the inner magnetosphere [*Lee and Takahashi*, 2006]. Persistent spatial features that are unique to the plasmasphere or trough could be examined in future statistical studies of the global distribution of MHD wave power if data from each region are studied separately. For example, *Brautigam et al.* [2005] found that electric field Pc5 PSDs decreased with decreasing radial distance. Our results suggest that part of this decrease is due to the presence of the plasmasphere at low L. In other words, the decrease at low L would not be as large if only trough data were studied.

[27] This study also suggests that radiation belt models that use empirical averages of Pc5 wave power should consider the location of the plasmapause. Radiation belt models that incorporate MHD waves as a source of radial diffusion could be improved by constraining the location of the plasmapause, since radial diffusion coefficients are affected by MHD wave power [*Elkington et al.*, 2003]. For example, an average for Pc5 power that included both trough and plasmasphere data would underestimate the average power in the trough. The effects of radial diffusion due to Pc5 waves would then be underestimated in the trough region.

References

Anderson, R. R., D. A. Gurnett, and D. L. Odem (1992), CRRES plasma wave experiment, *J. Spacecraft Rockets*, *29*(4), 570–573, doi:10.2514/3.25501.

Berube, D., M. B. Moldwin, and M. Ahn (2006), Computing magnetospheric mass density from field line resonances in a realistic magnetic field geometry, *J. Geophys. Res.*, *111*, A08206, doi:10.1029/2005JA011450.

Brautigam, D. H., G. P. Ginet, J. M. Albert, J. R. Wygant, D. E. Rowland, A. Ling, and J. Bass (2005), CRRES electric field power spectra and radial diffusion coefficients, *J. Geophys. Res.*, *110*, A02214, doi:10.1029/2004JA010612.

Chen, L., and A. Hasegawa (1991), Kinetic theory of geomagnetic pulsations: 1. Internal excitations by energetic particles, *J. Geophys. Res.*, *96*, 1503–1512, doi:10.1029/90ja02346.

Elkington, S. R., M. K. Hudson, and A. A. Chan (2003), Resonant acceleration and diffusion of outer zone electrons in an asymmetric geomagnetic field, *J. Geophys. Res.*, *108*(A3), 1116, doi:10.1029/2001JA009202.

Fraser, B. J., J. L. Horwitz, J. A. Slavin, Z. C. Dent, and I. R. Mann (2005), Heavy ion mass loading of the geomagnetic field near the plasmapause and ULF wave implications, *Geophys. Res. Lett.*, *32*, L04102, doi:10.1029/2004GL021315.

Hudson, M., R. Denton, M. Lessard, E. Miftakhova, and R. Anderson (2004), A study of Pc5 ULF oscillations, *Ann. Geophys.*, *22*(1), 289–302.

Johnson, M. H., and J. Kierein (1992), Combined release and radiation effects satellite (CRRES) - Spacecraft and mission, *J. Spacecraft Rockets*, *29*(4), 556–563, doi:10.2514/3.55641.

Kivelson, M. G., and D. J. Southwood (1985), Resonant ULF waves: A new interpretation, *Geophys. Res. Lett.*, *12*, 49–52, doi:10.1029/GL012i001p00049.

Lee, D.-H., and K. Takahashi (2006), MHD eigenmodes in the inner magnetosphere, in *Magnetospheric ULF Waves: Synthesis and New Directions, Geophys.Monogr. Ser.*, vol. 169, edited by K. Takahashi et al., pp. 73–89, AGU, Washington, D. C.

McIlwain, C. E. (1961), Coordinates for mapping the distribution of magnetically trapped particles, *J. Geophys. Res.*, *66*, 3681–3691, doi:10.1029/JZ066i011p03681.

Moldwin, M. B., L. Downward, H. K. Rassoul, R. Amin, and R. R. Anderson (2002), A new model of the location of the plasmapause: CRRES results, *J. Geophys. Res.*, *107*(A11), 1339, doi:10.1029/2001JA009211(Space Physics).

Samson, J. C., B. G. Harrold, J. M. Ruohoniemi, R. A. Greenwald, and A. D. M. Walker (1992), Field line resonances associated with MHD waveguides in the magnetosphere, *Geophys. Res. Lett.*, *19*, 441–444, doi:10.1029/92gl00116.

Singer, H. J., W. P. Sullivan, P. Anderson, F. Mozer, P. Harvey, J. Wygant, and W. McNeil (1992), Fluxgate magnetometer instrument on the CRRES, *J. Spacecraft Rockets*, *29*(4), 599–601, doi:10.2514/3.25506.

Takahashi, K., and B. J. Anderson (1992), Distribution of ULF energy (f is less than 80 mHz) in the inner magnetosphere: A statistical analysis of AMPTE CCE magnetic field data, *J. Geophys. Res.*, *97*, 10,751–10,773, doi:10.1029/92ja00328.

Takahashi, K., and A. Y. Ukhorskiy (2007), Solar wind control of Pc5 pulsation power at geosynchronous orbit, *J. Geophys. Res.*, *112*, A11205, doi:10.1029/2007JA012483.

Tsyganenko, N. A. (1989), A magnetospheric magnetic-field model with a warped tail current sheet, *Planet. Space Sci.*, *37*, 5–20, doi:10.1016/0032-0633(89)90066-4.

Wygant, J. R., P. R. Harvey, D. Pankow, F. S. Mozer, N. Maynard, H. Singer, M. Smiddy, W. Sullivan, and P. Anderson (1992), CRRES electric field/Langmuir probe instrument, *J. Spacecraft Rockets*, *29*(4), 601–604, doi:10.2514/3.25507.

R. R. Anderson, Physics and Astronomy Department, University of Iowa, Iowa City, IA 52242, USA.

V. Angelopoulos, M. Hartinger, and M. B. Moldwin, Earth and Space Sciences Department, University of California, Los Angeles, CA 90095, USA.

Y. Nishimura, Atmospheric and Oceanic Sciences Department, University of California, Los Angeles, CA 90095, USA.

H. J. Singer, NOAA Space Weather Prediction Center, 325 Broadway, Boulder, CO 80305, USA.

K. Takahashi, Johns Hopkins University Applied Physics Laboratory, Laurel, MD 20723, USA.

J. R. Wygant, School of Physics and Astronomy, University of Minnesota, Minneapolis, MN 55455, USA.